Supporting Information for:

Hemilability of the 1,2-Bis(dimethylphosphino)ethane (dmpe) Ligand in Cp*Mo(NO)(κ^2-dmpe)

Aaron S. Holmes, Brian O. Patrick, Taleah M. Levesque, and Peter Legzdins*

Department of Chemistry, The University of British Columbia, Vancouver, British Columbia, Canada V6T 1Z1.

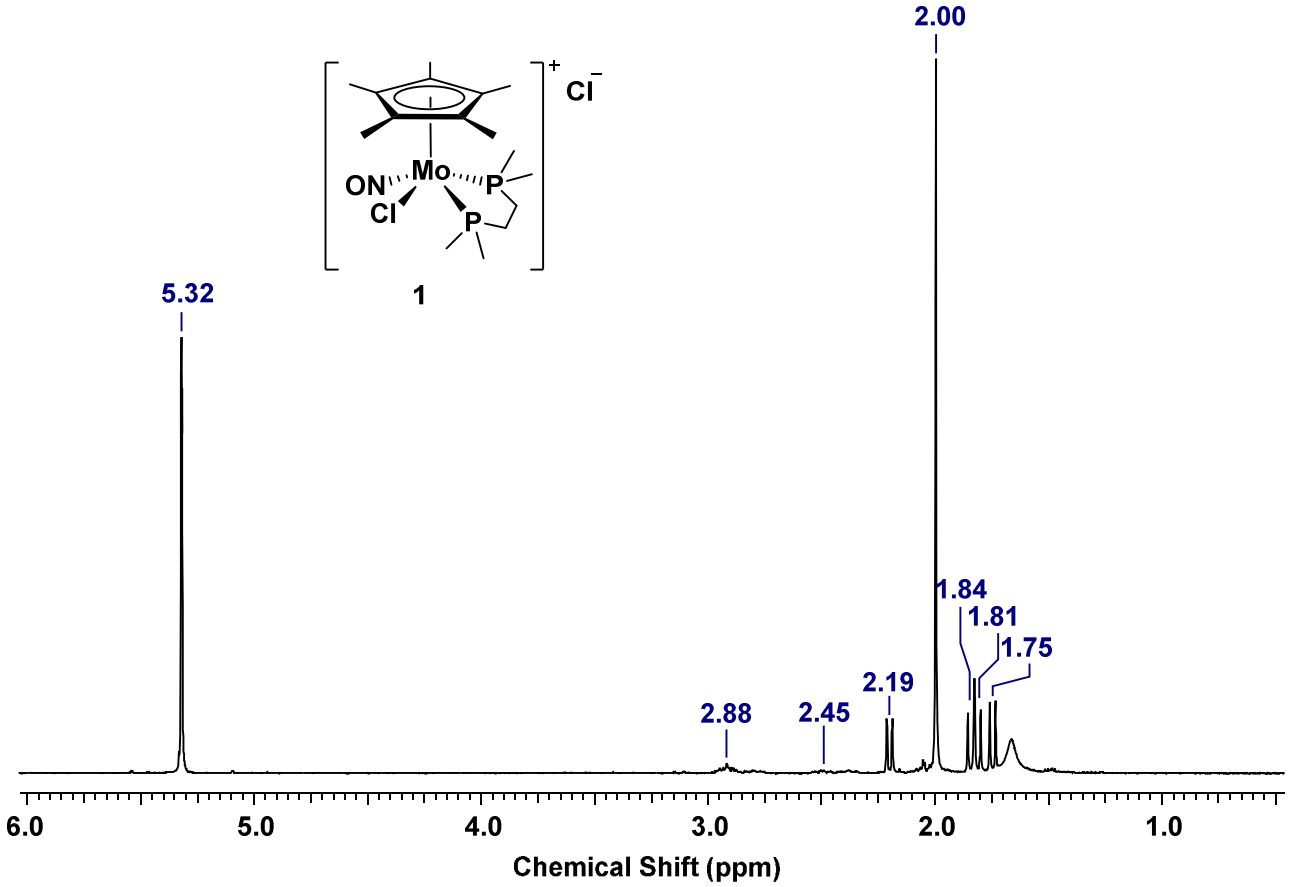

Figure S1. The ^{1}H NMR spectrum (400 MHz, CD_2Cl_2) of complex **1**.

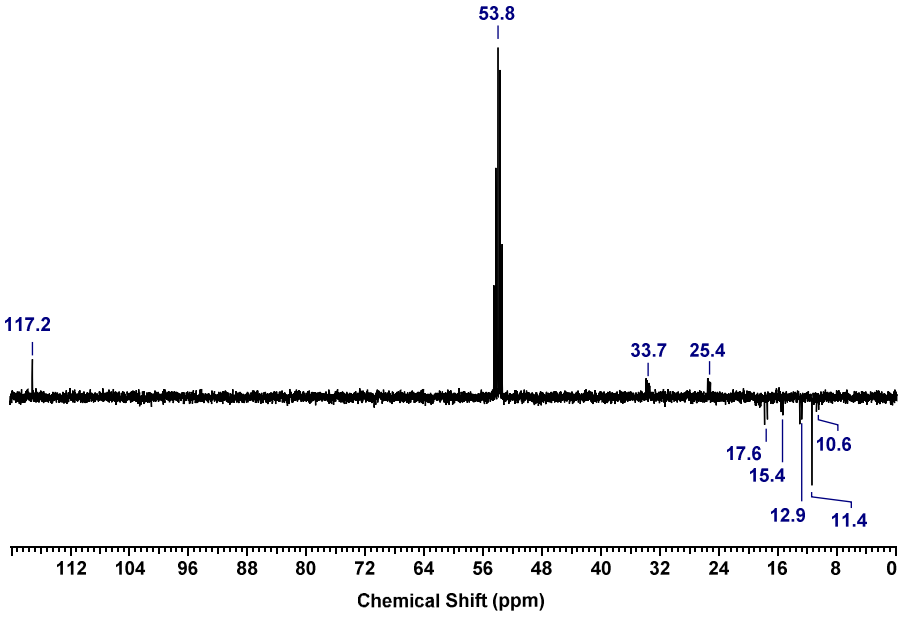

Figure S2. The ^{13}C APT NMR spectrum (100 MHz, CD_2Cl_2) of complex **1**.

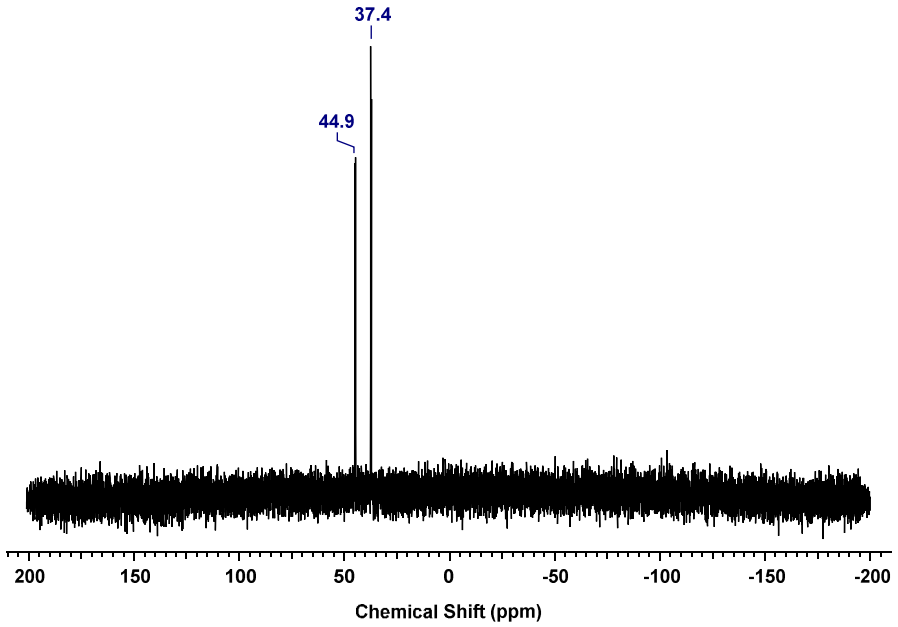

Figure S3. The $^{31}P\{^{1}H\}$ NMR spectrum (162 MHz, CD_2Cl_2) of complex **1**.

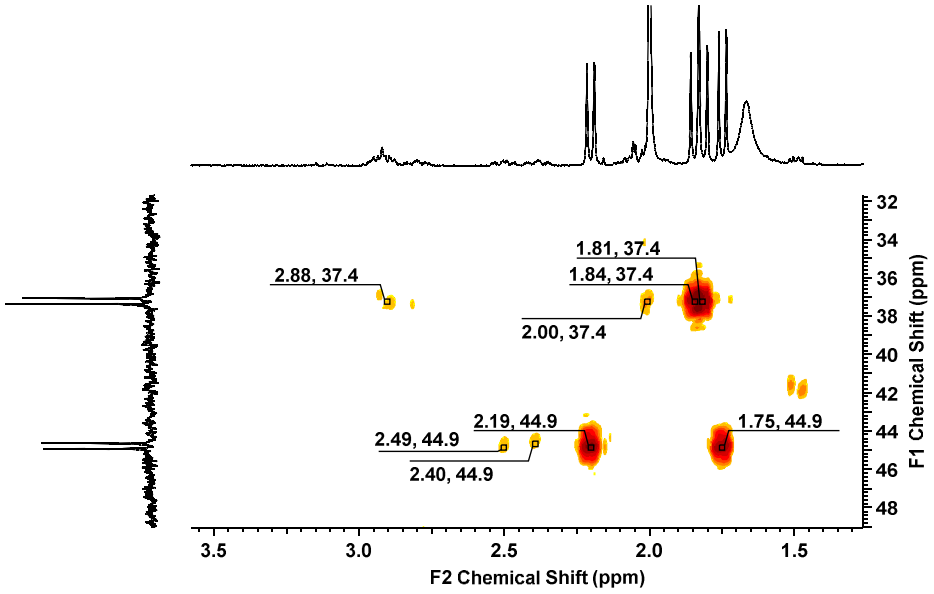

Figure S4. Expansion of the $\{^{1}H–^{31}P\}$ HMBC NMR spectrum (400 MHz, 162 MHz, C_6D_6) for complex **1** from δ 1.27 to 3.58 ppm on the F2 axis and δ 31.8 to 49.0 ppm on the F1 axis.

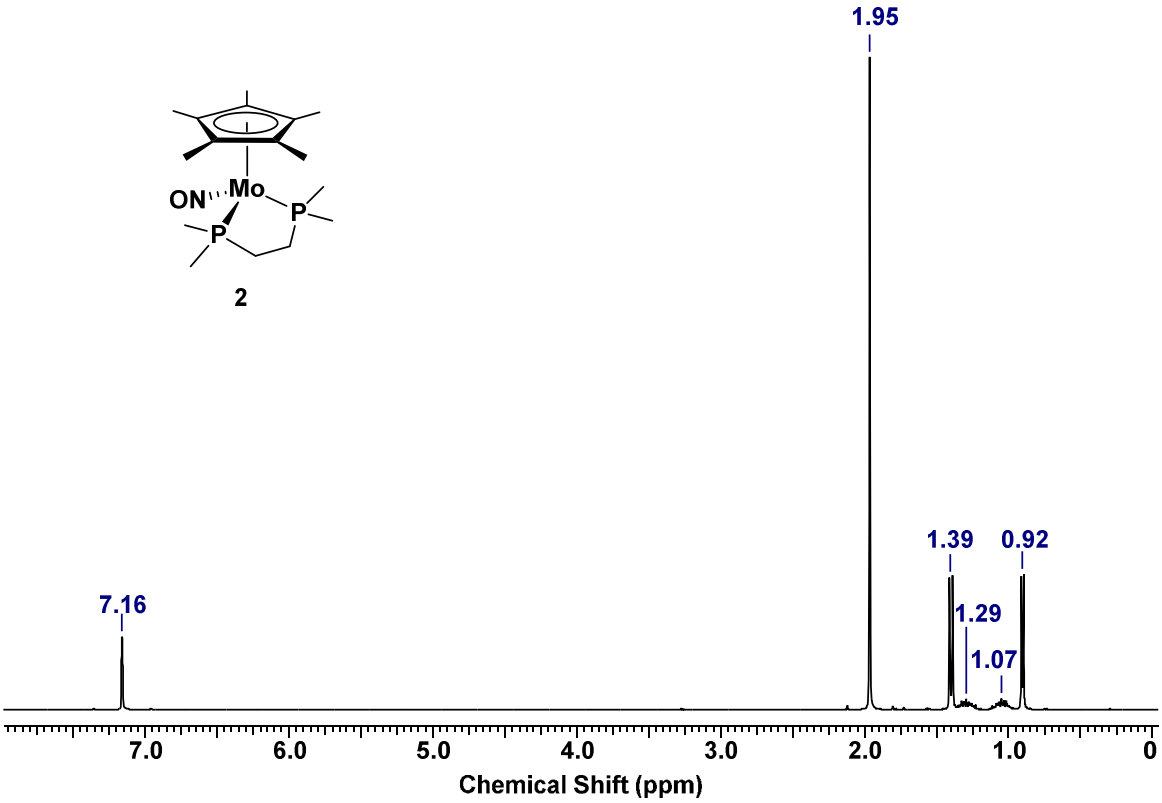

Figure S5. The ^{1}H NMR spectrum (400 MHz, C_6D_6) of complex **2**.

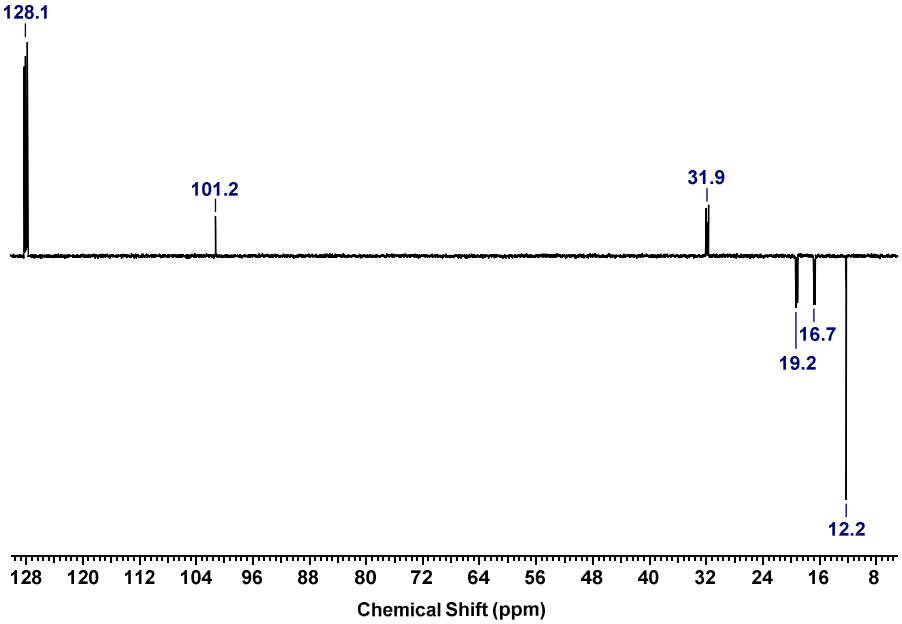

Figure S6. The ^{13}C APT NMR spectrum (100 MHz, C_6D_6) of complex **2**.

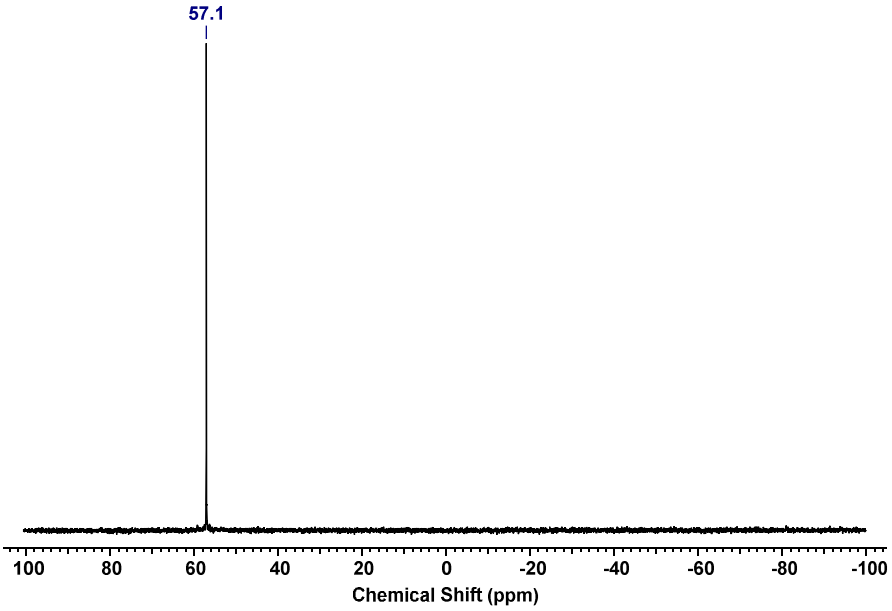

Figure S7. The $^{31}P\{^{1}H\}$ NMR spectrum (162 MHz, C_6D_6) of complex **2**.

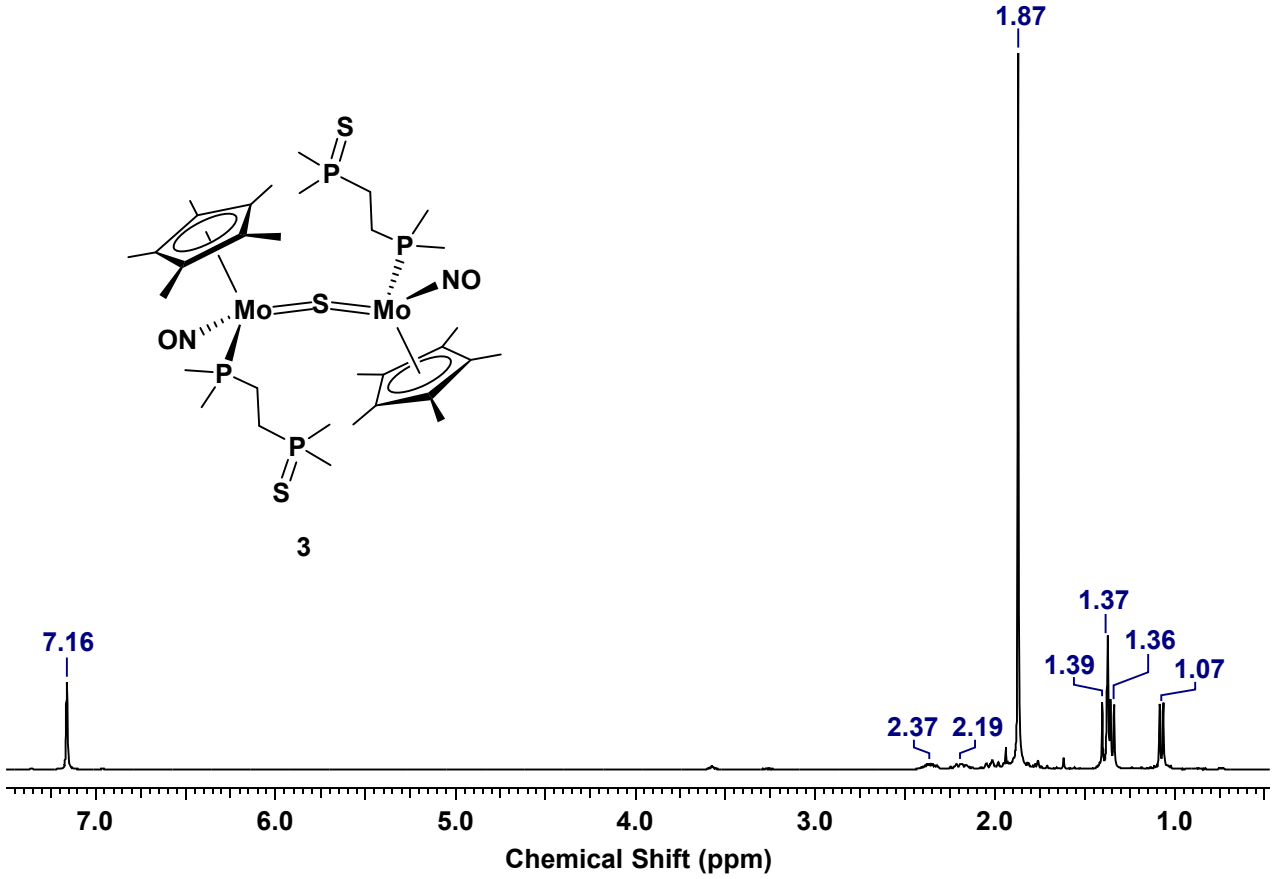

Figure S8. The ^{1}H NMR spectrum (400 MHz, C_6D_6) of complex **3**.

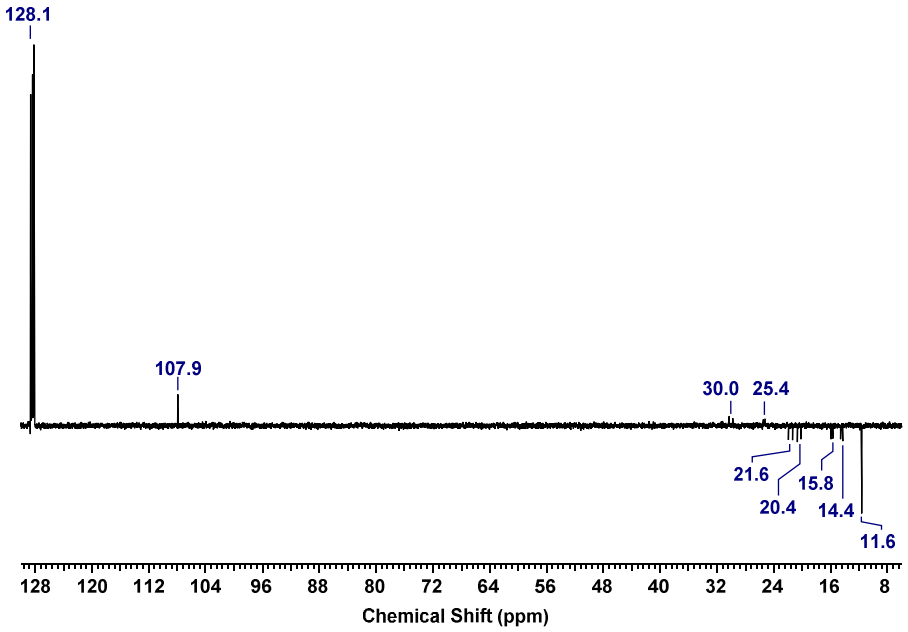

Figure S9. The ^{13}C APT NMR spectrum (100 MHz, C_6D_6) of complex **3**.

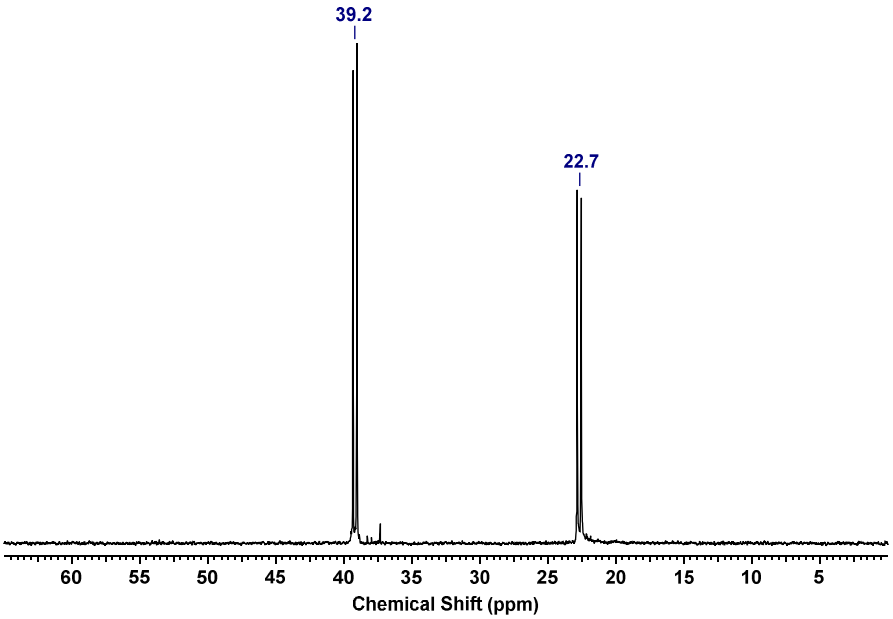

Figure S10. The $^{31}P\{^{1}H\}$ NMR spectra (162 MHz, C_6D_6) of complex **3**.

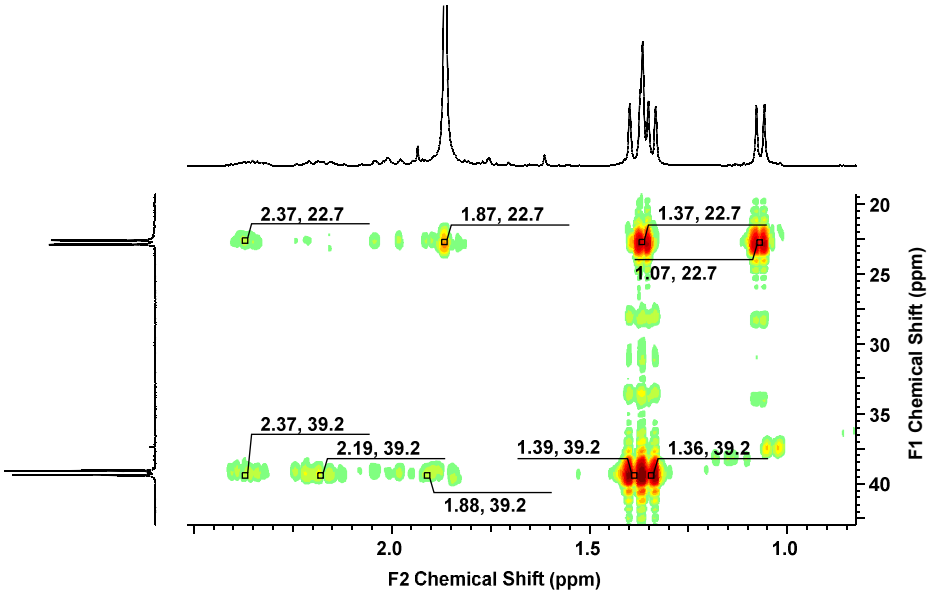

Figure S11. Expansion of the {^{1}H–^{31}P} HMBC NMR spectrum (400 MHz, 162 MHz, C_6D_6) for complex **3** from δ 0.83 to 2.51 ppm on the F2 axis and δ 19.5 to 42.5 ppm on the F1 axis.

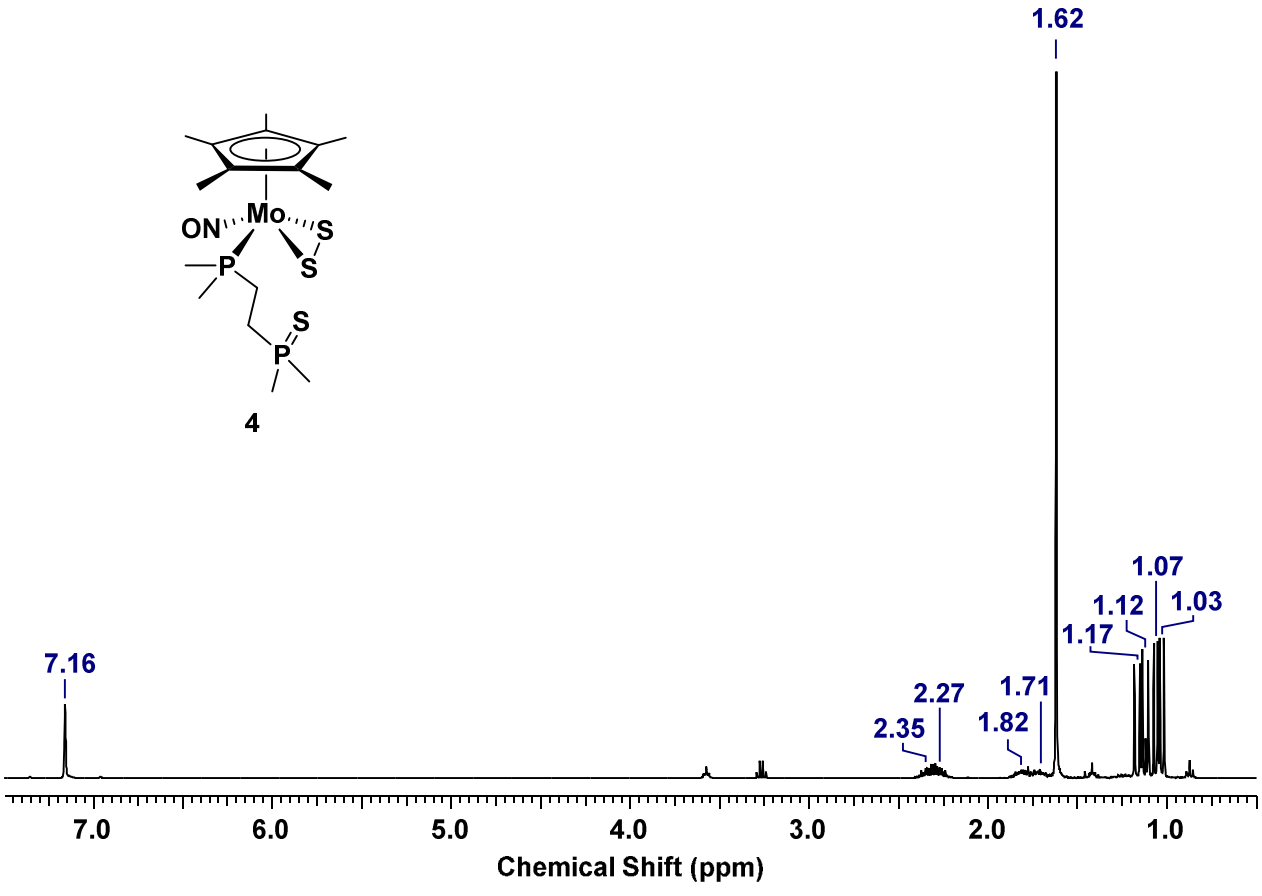

Figure S12. The ^{1}H NMR spectrum (400 MHz, C_6D_6) of complex **4**.

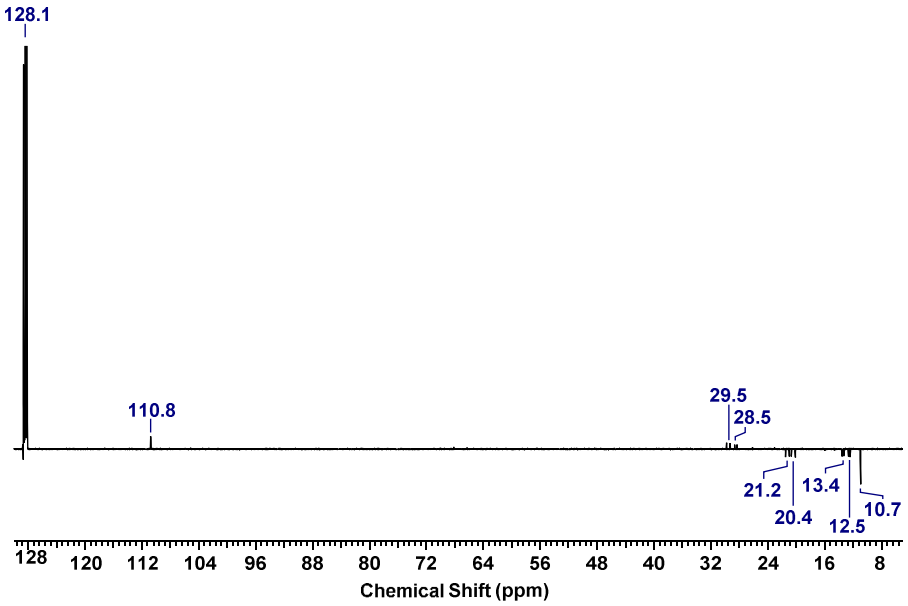

Figure S13. The ^{13}C APT NMR spectrum (100 MHz, C_6D_6) of complex **4**.

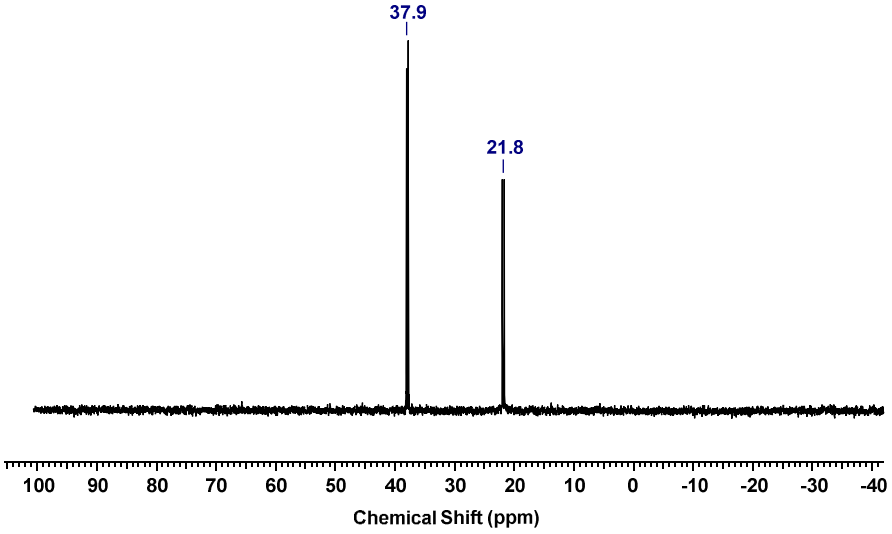

Figure S14. The $^{31}P\{^1H\}$ NMR spectrum (162 MHz, C_6D_6) of complex **4**.

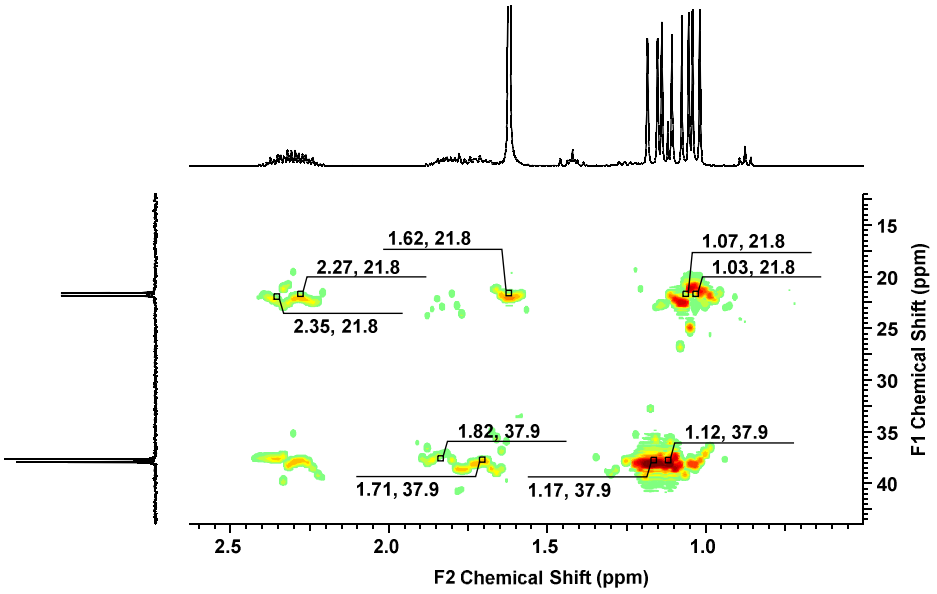

Figure S15. Expansion of the {^{1}H–^{31}P} HMBC NMR spectrum (400 MHz, 162 MHz, C_6D_6) for complex **4** from δ 0.50 to 2.63 ppm on the F2 axis and δ 12.0 to 43.6 ppm on the F1 axis.

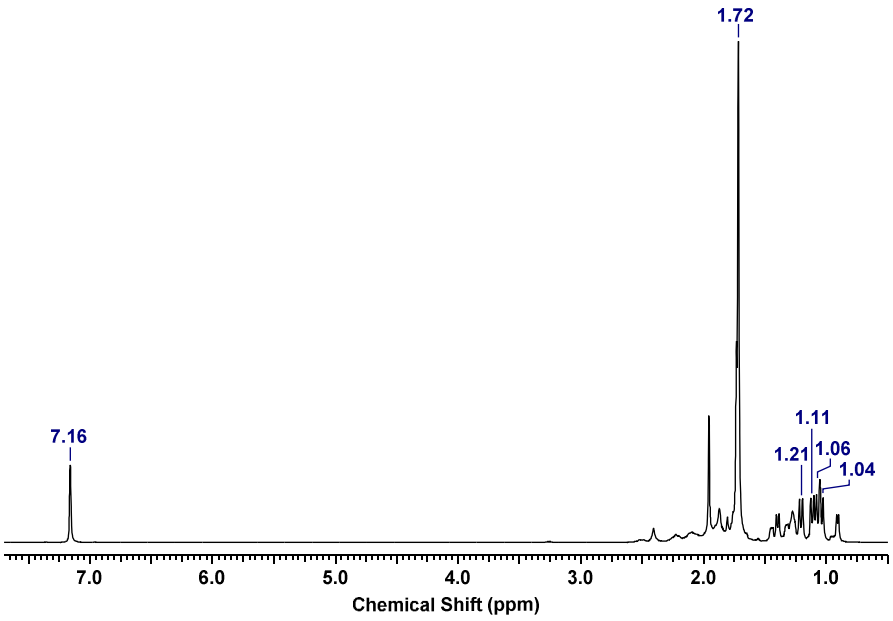

Figure S16. The ^{1}H NMR spectrum (400 MHz, C_6D_6) of the reaction mixture of complex **2** exposed to oxygen.

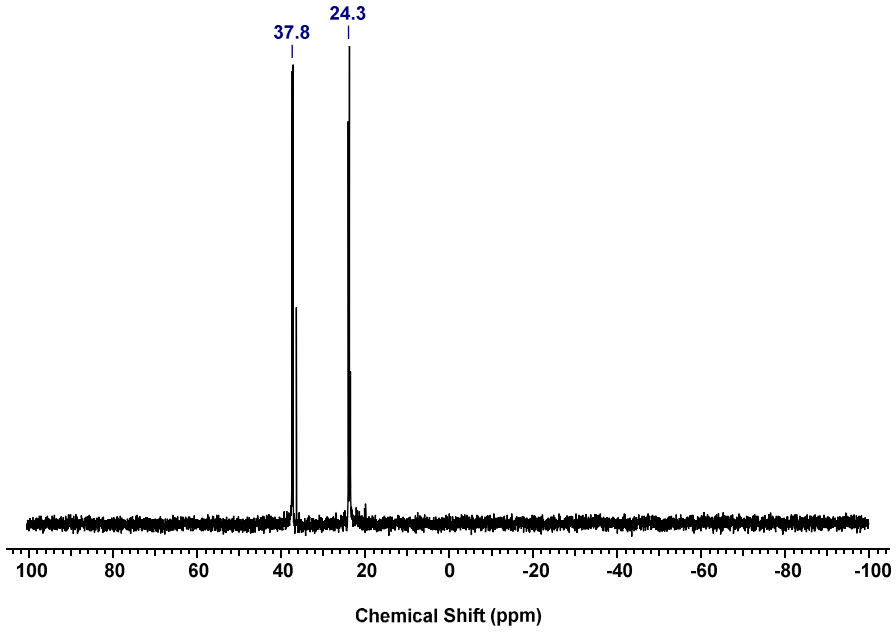

Figure S17. The $^{31}P\{^{1}H\}$ NMR spectrum (400 MHz, C_6D_6) of the reaction mixture of complex **2** after exposure to oxygen.

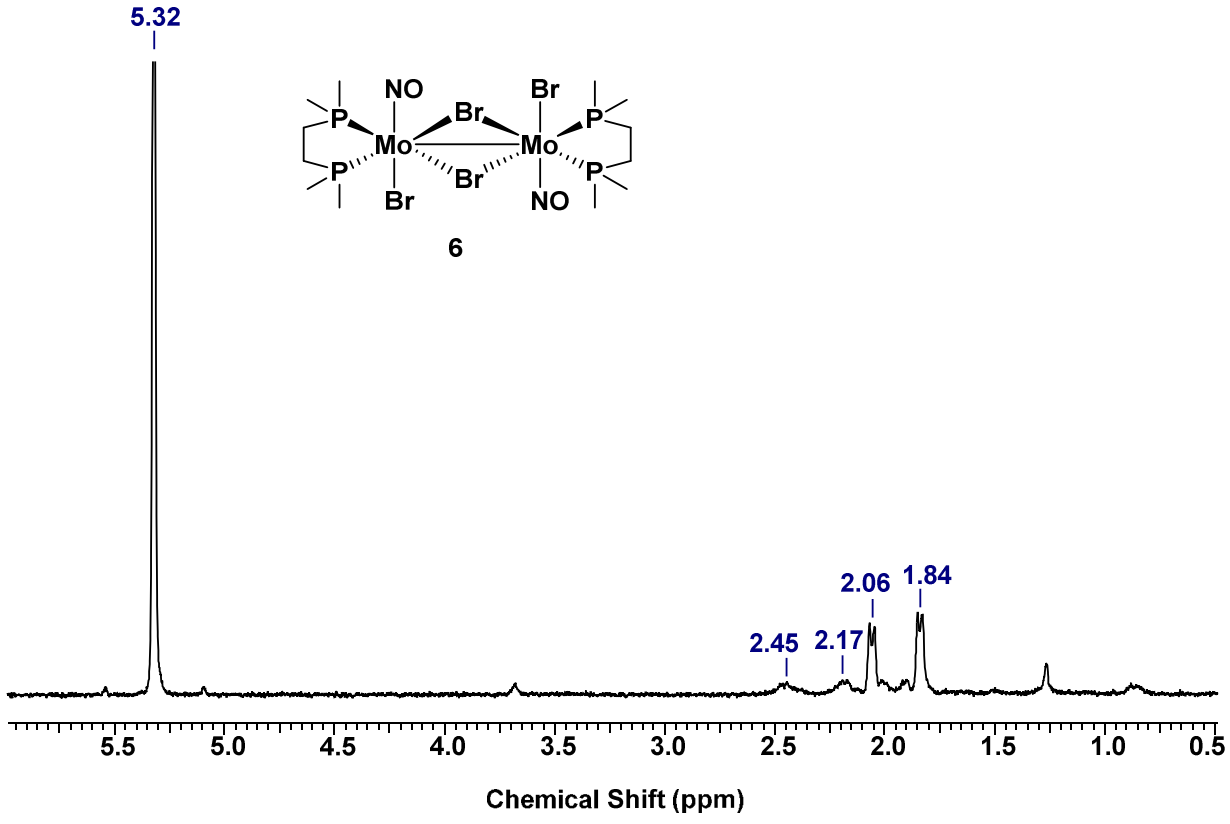

Figure S18. The ^{1}H NMR spectrum (400 MHz, CD_2Cl_2) of complex **6**.

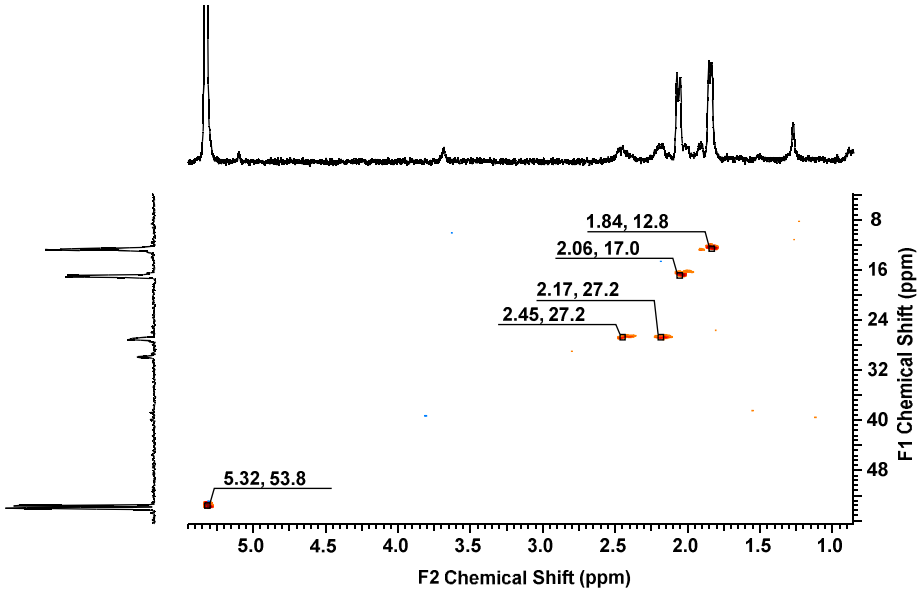

Figure S19. The $\{^{1}H–^{13}C\}$ HMBC NMR spectrum (400 MHz, 100 MHz, CD_2Cl_2) of complex **6**.

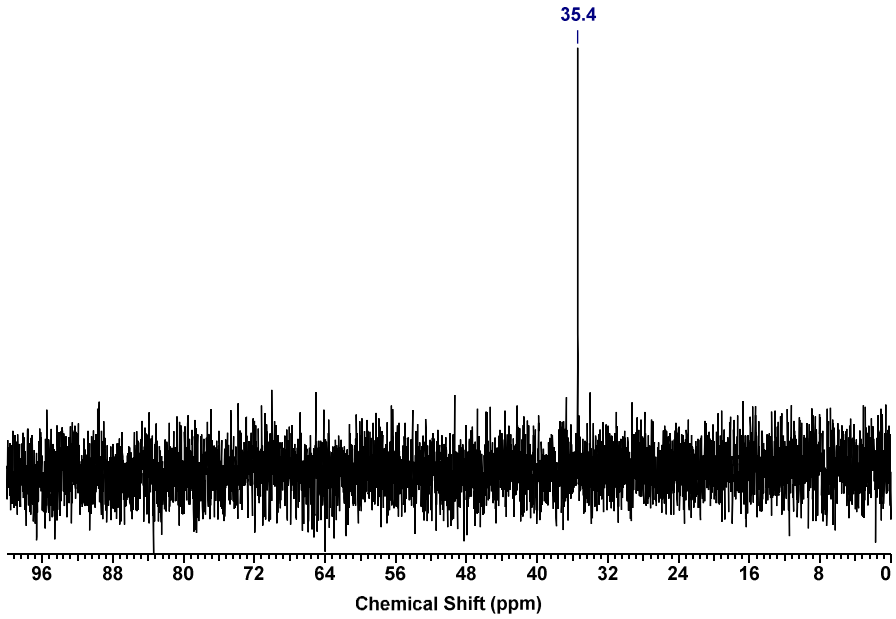

Figure S20. The $^{31}P\{^{1}H\}$ NMR spectrum (162 MHz, CD_2Cl_2) of complex **6**.

X-Ray Crystallography

Data collection was carried out at −173.0 ± 2 °C on a Bruker X8 APEX II diffractometer with cross-coupled multilayer optics using Mo-Kα radiation or at −183.0 ± 2 °C on a Bruker APEX DUO diffractometer equipped with a TRIUMPH curved-crystal monochromator using Mo-Kα radiation.

Data for **1** were collected to a maximum 2θ value of 60.1° in 0.5° oscillations using 20.0-second exposures. The crystal-to-detector distance was 50.16 mm. The material crystallizes as a two-component 'split-crystal' with components one and two related by a 3.9° rotation about the (1.00 0.642 0.000) direct crystal axis. Data were integrated for both twin components, including both overlapped and non-overlapped reflections. The structure was solved by direct methods[1] using non-overlapped data from the major twin component and expanded using Fourier techniques. Subsequent refinements were carried out using the same data set, containing all data from the major twin components. The material crystallizes with two water molecules and one free chloride in the asymmetric unit. All non-hydrogen atoms were refined anisotropically. All O−H hydrogen atoms were located in difference maps and refined isotropically. All other hydrogen atoms were included in calculated positions but not refined. The final cycle of full-matrix least-squares refinement was based on 6630 reflections and 251 variable parameters.

Data for **2** were collected to a maximum *2θ* value of 60.4° in 0.5° oscillations using 3.0-second exposures. The crystal-to-detector distance was 40.05 mm. The structure was solved by direct methods[1] and expanded using Fourier techniques. All non-hydrogen atoms were refined isotropically. All hydrogens atoms were placed in calculated positions. The final cycle of full-matrix least-squares refinement was based on 5650 reflections and 199 variable parameters.

Data for **3** were collected to a maximum 2θ value of 55.8° in 0.5° oscillations using 20.0-second exposures. The crystal-to-detector distance was 60.21 mm. The material crystallizes as a two-component 'split-crystal' with components one and two related by a 1.7° rotation about the (0.029 -0.003 1) direct crystal axis. Data were integrated for both twin components, including both overlapped and non-overlapped reflections. The structure was solved by direct methods[1] using non-overlapped data from the major twin component and expanded using Fourier techniques. The material crystallizes with one half-molecule in the asymmetric unit, with the bridging sulfur (S2) residing on a two-fold rotation axis. Subsequent refinements were carried out using a HKLF 5 format data set, containing all data from both twin components. All non-hydrogen atoms were refined anisotropically. All hydrogen atoms were included in calculated positions but not refined. The final cycle of full-matrix least-squares refinement was based on 11361 reflections and 214 variable parameters.

Data for **4** were collected to a maximum 2θ value of 50.8° in 0.5° oscillations using 60.0-second exposures. The crystal-to-detector distance was 40.18 mm. The material crystallizes as a two-component 'split-crystal' with components one and two related by a 3.5° rotation about the (1 0.100 0.013) direct crystal axis. Data were integrated for both twin components, including both overlapped and non-overlapped reflections. The structure was solved by direct methods[1] using non-overlapped data from the major twin component and expanded using Fourier techniques. The material crystallizes with significant disorder. The Cp* ring, the disulfide group and two methyl groups are disordered and were modeled in two orientations. Subsequent refinements were carried out using a HKLF 4 format data set, containing all data from component one. All non-hydrogen atoms were refined anisotropically. All hydrogen atoms

were included in calculated positions but not refined. The final cycle of full-matrix least-squares refinement was based on 4106 reflections and 337 variable parameters.

Data for **5** were collected to a maximum 2θ value of 60.2° in 0.5° oscillations using 10.0-second exposures. The crystal-to-detector distance was 50.22 mm. The structure was solved by direct methods.[1] The material crystallizes with one half-molecule in the asymmetric unit, related to the other half-molecule by an inversion centre at (1−X, −Y, 1−Z). Additionally, there is significant disorder of the coordination around the Mo center, with one bromine and the nitrosyl swapping positions. The bridging P-ligand is also disordered in two orientations. All non-hydrogen atoms were refined isotropically. All hydrogens atoms were placed in calculated positions. The scattering data and disorder make it impossible to locate hydrides on either Mo atom. The final cycle of full-matrix least-squares refinement on F2 was based on 5103 reflections and 238 variable parameters.

Data for **6** were collected to a maximum 2θ value of 60.1° in 0.5° oscillations using 4.0-second exposures. The crystal-to-detector distance was 40.11 mm. The material crystallizes as a two-component twin with components one and two related by a 179.6° rotation about the (1 0 1) reciprocal axis. Data were integrated for both components, including both overlapped and non-overlapped reflections. The structure was solved by direct methods[1] using non-overlapped data from the major twin component. Subsequent refinements were carried out using an HKLF 4 format data set containing complete data from component one. The molecule crystallizes with one half-molecule in the asymmetric unit, related to the other by an inversion centre at (1−X, 1−Y, 1−Z). Additionally, the bromo and nitrosyl substituents are positionally disordered in a 50/50 ratio. All non-hydrogen atoms were refined anisotropically. All hydrogen atoms were

placed in calculated positions. The final cycle of full-matrix least-squares refinement was based on 3813 reflections and 139 variable parameters.

Neutral atom scattering factors were taken from Cromer and Waber.[2] Anomalous dispersion effects were included in Fcalc;[3] the values for Δf' and Δf'' were those of Creagh and McAuley.[4] The values for the mass attenuation coefficients are those of Creagh and Hubbell.[5] All refinements were performed using the SHELXL-2014[6] via the OLEX2[7] interface.

Table S1. X-ray crystallographic data for complexes **1**, **2**, and **3**.

Complex	**1**	**2**	**3**
Empirical Formula	$C_{16}H_{31}MoNOP_2Cl_2$•2 H_2O	$C_{16}H_{31}MoNOP_2$	$C_{32}H_{62}Mo_2N_2O_2P_4S_3$
Formula Weight	518.23	411.30	918.77
Crystal Colour, Habit	yellow, needle	orange, irregular	blue, blade
Crystal Size (mm)	0.02 × 0.08 × 0.22	0.12 × 0.21 × 0.23	0.07 × 0.18 × 0.45
Crystal System	triclinic	orthorhombic	monoclinic
Space Group	P_{-1}	*Pbca*	*C*2/*c*
Volume (Å^3)	1130.49(10)	3824.9(4)	4444.2(4)
a (Å)	8.8393(4)	13.6802(9)	22.7280(10)
b (Å)	9.4840(5)	16.4231(11)	11.9139(5)
c (Å)	15.0666(7)	17.0245(12)	19.5595(10)
α (°)	86.290(3)	90	90
β (°)	84.030(3)	90	122.913(3)
γ (°)	64.175(3)	90	90
Z	2	8	4
Density, ρ (calculated) (g/cm^3)	1.522	1.428	1.373
Absorption Coefficient, μ (mm^{-1})	0.973	0.852	0.877
F_{000}	536	1712	1904
Measured Reflections: Total	50330	47214	33932
Measured Reflections: Unique	6630	5650	11361
Final R Indices[a]	R_1 = 0.036 wR_2 = 0.094	R_1 = 0.020 wR_2 = 0.047	R_1 = 0.042 wR_2 = 0.117
Goodness-of-fit on F^{2,b}	1.10	1.05	1.02
Largest diff. peak/hole (e$^-$Å^{-3})	2.09/−0.98	0.45/−0.29	2.23/−0.71

[a]R1 on F = $\sum\left||F_o| - |F_c|\right| / \sum|F_o|$; wR2 = $\sqrt{\sum\left(\left({F_o}^2 - {F_c}^2\right)^2\right) / \sum w\left({F_o}^2\right)^2}$; w = $\left(\sigma^2{F_o}^2\right)^{-1}$

[b]GOF = $\sqrt{\sum(w\,(|F_o| - |F_c|)^2) \,/\, degrees\ of\ freedom}$

Table S2. X-ray crystallographic data for complexes **4**, **5**, and **6**.

Complex	**4**	**5**	**6**
Empirical Formula	$C_{16}H_{31}MoNOP_2S_3$	$C_{26}H_{46}Br_4Mo_2N_2O_2P_2$	$C_{12}H_{32}Mo_2N_2O_2P_4Br_4$
Formula Weight	507.48	992.11	871.79
Crystal Colour, Habit	red, plate	orange, needle	red, plate
Crystal Size (mm)	0.02 × 0.12 × 0.25	0.07 × 0.14 × 0.35	0.09 × 0.18 × 0.20
Crystal System	triclinic	monoclinic	monoclinic
Space Group	P_{-1}	$P2_1/n$	$P2_1/n$
Volume (Å^3)	1121.45(18)	1735.5(4)	1308.82(11)
a (Å)	9.4988(9)	8.1677(11)	9.1639(4)
b (Å)	9.5065(9)	13.4105(19)	13.4852(7)
c (Å)	13.0367(12)	15.846(2)	10.6579(5)
α (°)	98.361(5)	90	90
β (°)	100.551(4)	90.937(2)	96.416(1)
γ (°)	99.770(5)	90	90
Z	2	2	2
Density, ρ (calculated) (g/cm^3)	1.503	1.899	2.212
Absorption Coefficient, μ (mm^{-1})	1.011	5.445	0.732
F_{000}	524	972	836
Measured Reflections: Total	27459	18823	23972
Measured Reflections: Unique	4106	5103	3813
Final R Indices[a]	R_1 = 0.056 wR_2 =0.166	R_1 = 0.054 wR_2 = 0.118	R_1 = 0.061 wR_2 = 0.118
Goodness-of-fit on F^2[,b]	1.10	1.03	1.33
Largest diff. peak/hole (e$^-$Å^{-3})	1.70/−1.04	1.94/−1.23	1.43/−1.47

[a]R1 on F = $\sum\left||F_o| - |F_c|\right| / \sum|F_o|$; wR2 = $\sqrt{\sum\left(\left({F_o}^2 - {F_c}^2\right)^2\right) / \sum w\left({F_o}^2\right)^2}$; w = $\left(\sigma^2{F_o}^2\right)^{-1}$

[b]GOF = $\sqrt{\sum(w\,(\,|F_o| - |F_c|\,)^2) \,/\, degrees\ of\ freedom}$

REFERENCES

(1) Sheldrick, G. M. *SHELXT* - Integrated Space-group and Crystal-structure Determination. *Acta Crystallogr.* **2015**, *A71*, 3-8.

(2) Cromer, D. T.; Waber, J. T. *International Tables for X-ray Crystallography*; The Kynoch Press: Birmingham, 1974; Vol. IV, Table 2.2 A.

(3) Ibers, J. A.; Hamilton, W. C. Dispersion Corrections and Crystal Structure Refinements. *Acta Crystallogr*. **1964**, *17*, 781-782.

(4) Creagh, D. C.; McAuley, W. J. *International Tables for X-ray Crystallography*; Kluwer Academic Publishers: Boston, 1992; Vol. C., Table 4.2.6.8, pp 219-222.

(5) Creagh, D. C.; Hubbell, J. H. *International Tables for X-ray Crystallography*; Kluwer Academic Publishers: Boston, 1992; Vol. C., Table 4.2.4.3, pp 200-206.

(6) Sheldrick, G. M. Crystal Structure Refinement with *SHELXL*. *Acta Crystallogr.* **2015**, *C71*, 3-8.

(7) Dolomanov, O. V.; Bourhis, L. J.; Gildea, R. J.; Howard, J. A. K.; Puschmann, H. *OLEX2*: A Complete Structure Solution, Refinement and Analysis Program. *J. Appl. Crystallogr.* **2009**, *42*, 339-341.